



Estimation of SNR Including Quantization Error of Multi-Wavelength Lidar Receiver

Zena A. Abed*

Muna M. Hummady**

*,***Department of Information and Communication Engineering/ AL-Khwarizmi College of Engineering/ University of Baghdad*

*Email: baghdad_zaa@yahoo.com

**Email: muna_hummady@yahoo.com

(Received 12 November 2012; Accepted 23 April 2013)

Abstract

This paper comprises the design and operation of mono-static backscatter lidar station based on a pulsed Nd: YAG laser that operates at multiple wavelengths. The three-color lidar laser transmitter is based on the collinear fundamental 1064 nm, second harmonic 532 nm and a third harmonic 355nm output of a Nd:YAG laser. The most important parameter of lidar especially daytime operations is the signal-to-noise ratio (SNR) which gives some instructions in designing of lidar and it is often limit the effective range. The reason is that noises or interferences always badly affect the measured results. The inversion algorithms have been developed for the study of atmospheric aerosols. Signal-to-noise ratio (SNR) of three-color channel receivers were presented while averaging together 1, 20, 50 and 100 lidar returns and combined to the signal to noise ratio associated with the quantization process for each channel.

Keywords: *lidar, Signal-to-noise ratio, aerosols, noise, laser radar.*

1. Introduction

LIDAR is an acronym of (Light Detection and Ranging); it works on the same principal as ordinary (radar), except that light is used instead of radio waves.

The basic principles are similar, i.e. a short pulse of light is transmitted, scatters from an object and returns to the receiver. In atmosphere, the lidar pulse is scattered from molecules which are small compared to the wavelength of the radiation (Rayleigh or Raman scattering), from particles of dust or aerosols with sizes on the order of the wavelength of the radiation or larger (Mie scattering). This process is important in the lower regions of the atmosphere (from the ground to about 25 km) where dust and aerosols are significant components of the atmosphere, or from pieces at specific wavelengths (resonance fluorescence) [1,2].

This paper comprises the computational assessment of an elastic lidar system based on a

pulsed Nd: YAG laser that operates at multiple wavelengths (355,532 and 1064nm) for retrievals of troposphere aerosol, cloud characteristic and water vapor vertical profiles.

2. Description of Multi-Wavelength Lidar Instrument

The design of the lidar instrument presented in this paper is based on the authors design of several previous lidar systems with several key exceptions [3].

The lidar instrument presented here makes use of three wavelengths of light, and is specifically designed to study atmospheric aerosols. Important design considerations specific to aerosol study are that the laser beam and the telescope field of view (FOV) are fully overlapped (the laser beam transverse energy profile fits within the telescope field of view) at ranges where aerosols are to be

studied, and that each detector (there is one detector for each of the three wavelengths of light) sees the same field of view.

Additionally, the vertical resolution, which is determined primarily by the laser pulse-width, should be small enough to reasonably observe atmospheric aerosols. Other design parameters of note are that the laser should emit enough energy per pulse to adequately illuminate the atmosphere, and that background light from the sky is somehow prevented (as much as possible) from striking the optical detectors.

As the light source for the three-wavelength lidar instrument, Nd:YAG laser was chosen because fundamental, second and third harmonic frequencies emitted by such a laser are adequate for studying atmospheric aerosols, and optical components optimized for their harmonic wavelengths are relatively easy and economical to obtain [4].

A schematic of the three-wavelength lidar instrument is shown in Fig. 1. The lidar transmitter is 20 Hz Q-switched Nd: YAG laser. It produce light at the fundamental 1064 nm, second harmonic 532nm, and third harmonic 355 wavelengths. The laser beams are expanded and re-collimated using a diverging lens and incident on a dielectric mirrors that direct most of the collinear fundamental, second and third harmonic light into the atmosphere.

The optical receiver for the three-color lidar instrument uses a 28 cm diameter Schmidt-Cassegrain telescope to collect the light scattered by the atmosphere. Since the optical power received by a lidar system is proportional to the physical area of the light collection optics, using as large a telescope as practicable is advantageous [5].

A gated PMT is used to monitor the 532 nm and 355 nm channels while an APD is used to monitor the 1064 nm channel. The electrical signals from the APD and PMT assemblies are digitized using a 14 bit 200 MHz A/D converter [5].

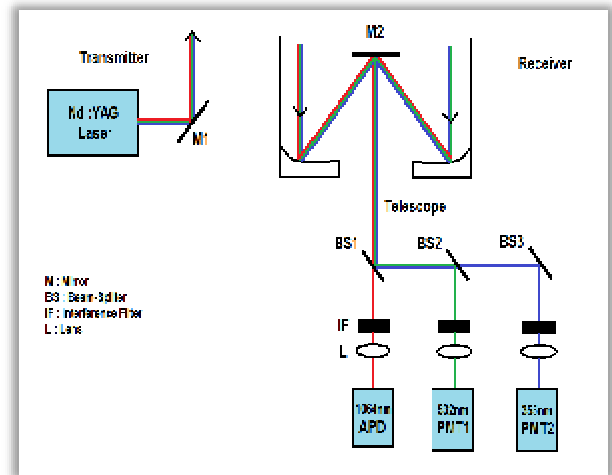


Fig. 1. Schematic Diagram of Three-Color Lidar Instrument.

3. Solving Lidar Equation (Retrieval Method)

The lidar equation can be derived using the Mie theory of scattering [6]. The equation defining the backscattered power received by a lidar system at any given time can be represented as a function of the light transmitted by the lidar attenuated by various factors and delayed by the round-trip travel time of that light, can be expressed as:

$$p(R) = p_t \frac{\pi D_{rec}}{R^2} \frac{c \tau}{2} \beta(r) e^{-2 \int_0^R \sigma(R') dr'} \epsilon(\lambda) \epsilon(R) t \dots(1)$$

where p_t is the laser transmitter pulse power in Watts, D_{rec} is the receiver optics diameter in m, c is the speed of light in m/s, τ is the laser pulse duration in seconds, $\beta(R)$ is the backscatter coefficient with units of $(\frac{1}{m \cdot sr})$, $\sigma(R)$ is the extinction coefficient with units of $(\frac{1}{m \cdot sr})$, $\epsilon(\lambda)$ is the spectral transmission of the receiver optics at wavelength λ and $\epsilon(R)$ is the overlap function and is unitless.

The overlap function, $\epsilon(R)$, refers to the overlap between the field of view of the telescope and the intensity profile of the laser as a function of range.

The lidar inversion for the data collected with the two color lidar is based on methods developed by Fernald et al [7]. Taking into account multiple transmitter wavelengths, Eq (1) can be re-written as:

$$p_{\lambda}(R) = p_{t,\lambda} \frac{\pi D_{rec}}{R^2} \frac{c \tau}{2} \beta(\lambda, R) e^{-2 \int_0^R \sigma(\lambda, R) dR'} \epsilon(\lambda) \epsilon(R) \quad \dots(2)$$

and describes the amount of light received by the detectors from range bin R for a given wavelength λ . If all of the constants that are unique to the particular instrument for a particular wavelength are combined into one constant c_{λ} where:

$$C_{\lambda} = \frac{\pi D_{rec} c \tau}{2} \epsilon(\lambda) \epsilon(R) \quad \dots(3)$$

and the round trip atmospheric transmission is:

$$T^2(\lambda, R) = e^{-2 \int_0^R \sigma(\lambda, R) dR'} \quad \dots(4)$$

Eq (2) can be written as:

$$p_{\lambda}(R) = \frac{p_{t,\lambda} C_{\lambda} \beta(\lambda, R) T^2(\lambda, R)}{R^2} \quad \dots(5)$$

The assumption that the lidar inversion will only be completed when the lidar transmitter and the optical receiver are in full overlap allows as writing the overlap function $\epsilon(\mathbf{r}) = 1$.

The two components, model of the atmosphere takes into account Mie scattering from atmospheric aerosols and Rayleigh scattering from atmospheric molecules. As described by Wang et al. [8], the backscatter coefficient can be written in terms of these atmospheric scattering components as:

$$\beta(\lambda, R) = \beta_A(\lambda, R) + \beta_{RM}(\lambda, R) \quad \dots(6)$$

where $\beta_A(\lambda, \mathbf{r})$ is the backscatter coefficient is associated with the atmospheric aerosols and $\beta_{RM}(\lambda, \mathbf{R})$ is the backscatter coefficient associated with the atmospheric molecules.

Similarly, the extinction coefficient can be written as [8]:

$$\sigma(\lambda, R) = \sigma_A(\lambda, R) + \sigma_{RM}(\lambda, R) \quad \dots(7)$$

where $\sigma_A(\lambda, \mathbf{R})$ is the extinction coefficient associated with the atmospheric aerosols and $\sigma_{RM}(\lambda, \mathbf{R})$ is the extinction coefficient associated with the atmospheric molecules.

The relationship between the aerosol extinction and the aerosol backscatter is written as $S_A(\lambda) = \frac{\sigma_A(\lambda, R)}{\beta_A(\lambda, R)}$ and is known as lidar ratio. An equivalent lidar ratio can be written for the molecular backscatter and extinction as $S_{RM}(\lambda) = \frac{\sigma_{RM}(\lambda, R)}{\beta_{RM}(\lambda, R)}$.

The lidar ratio is assumed to be constant with altitude and it is essential to this inversion technique. The assumption of the constant lidar

ratio allows the total atmospheric transmission to be written as [8]:

$$T^2(\lambda, R) = T_A^2(\lambda, R) T_{RM}^2(\lambda, R) \quad \dots(8)$$

The atmospheric transmission due to atmospheric aerosols is:

$$T_A^2(\lambda, R) = e^{-2 S_A(\lambda) \int_0^R \beta_A(\lambda, R) dR'} \quad \dots(9)$$

and that the atmospheric transmission due to molecules is:

$$T_{RM}^2(\lambda, R) = e^{-2 S_{RM}(\lambda) \int_0^R \beta_{RM}(\lambda, R) dR'} \quad \dots(10)$$

The molecular backscatter and extinction coefficients associated with the Rayleigh scatter can be modeled. The molecular backscatter is given by:

$$\beta_{RM}(\lambda, R) = \left(374.28 \left(\frac{P(h)}{T(h)} \right) \right) / \lambda^4 \quad \dots(11)$$

Where λ is given in nm and $\beta_{RM}(\lambda, \mathbf{R})$ is given in $(\text{m.s})^{-1}$, $T(h)$ is the temperature in Kelvin written as a function of height and h is the height above mean sea level given in meters.

The temperature as a function of altitude h for 0 to 11 km can be modeled as [8]:

$$T(h) = 288.15 - 0.00654h \quad \dots(12)$$

The pressure over the same altitude range can be modeled as [9]:

$$P(h) = 1.013 \times 10^5 \left(\frac{288.15}{T(h)} \right)^{-5.2199} \quad \dots(13)$$

Where the pressure, $P(h)$ is given in Pascal.

Knowing the molecular backscatter allows the molecular extinction to be calculated by using $S_{RM}(\lambda) = \frac{8\pi}{3}$.

If the two components atmosphere model is applied to Eqs (7, 8 and 10), the lidar equation for a two component atmosphere can be written as:

$$P_{\lambda}(R) = \frac{P_{t,\lambda} C_{\lambda} [\beta_A(\lambda, R) + \beta_{RM}(\lambda, R)] T_A^2(\lambda, R) T_{RM}^2(\lambda, R)}{R^2} \quad \dots(14)$$

By solving Eq (14) for the aerosol backscatter coefficient, $\beta_A(\lambda, \mathbf{R})$ using the techniques presented in [7], the lidar inversion can then be completed.

Taking the derivative of Eq (9) with respect to r yields:

$$\frac{dT_A^2(\lambda, R)}{dR} = -2 S_A(\lambda) \beta_A(\lambda, R) T_A^2(\lambda, R) \quad \dots(15)$$

Solving Eq (14) for $\beta_A(\lambda, R)$ and substituting into Eq (15) yields the first order differential equation [7].

$$\frac{dT_A^2(\lambda, R)}{dR} - 2S_A(\lambda) \beta_A(\lambda, R) T_A^2(\lambda, R) = \frac{2S_A(\lambda) R^2 P_\lambda(R)}{P_{t,\lambda} C_\lambda T_{RM}^2(\lambda, R)} \quad \dots(16)$$

This first order differential equation in T_A^2 can be solved using the standard solution to get the transmission due to the aerosols.

$$T_A^2(\lambda, R) = e^{2S_A(\lambda) \int_0^R \beta_{RM}(\lambda, R') dR'} \times \left(1 - \frac{2S_A(\lambda)}{C_\lambda} \int_0^R \frac{R'^2 P_\lambda(R')}{P_{t,\lambda} T_{RM}^2(\lambda, R')} e^{-2S_A(\lambda) \int_0^{R'} \beta_{RM}(\lambda, R'') dR''} dR' \right) \quad \dots(17)$$

If a range corrected return is written as:

$$L_\lambda(R) = R^2 P_\lambda(R) \quad \dots(18)$$

and combined with the substitution of Eq (17) and Eq (10) into Eq (14) the result is an equation which solves for the aerosol backscatter.

$$\beta_A(\lambda, R) - \beta_{RM}(\lambda, R) + \left(\frac{L_\lambda(R) e^{-2(S_A(\lambda) - S_{RM}(\lambda)) \int_0^R \beta_{RM}(\lambda, R') dR'}}{C_\lambda P_{t,\lambda} T^2(R) - 2S_A(\lambda) \int_0^R \frac{L_\lambda(R')}{T_{RM}^2(\lambda, R')} e^{-2S_A(\lambda) \int_0^{R'} \beta_{RM}(\lambda, R'') dR''} dR'} \right) \quad \dots(19)$$

The outgoing laser pulse and the telescope field of view are not in full overlap at altitudes below approximately 0.5 km; Eq (19) must be slightly modified. This is done by having the lidar inversion take place over a range from some r_0 to r rather than from 0 to r [7, 8]. If the laser and telescope come into full overlap at r_0 then Eq (19) is modified to instead be.

$$\beta_A(\lambda, R) = -\beta_{RM}(\lambda, R) + \left(\frac{L_\lambda(R) e^{-2(S_A(\lambda) - S_{RM}(\lambda)) \int_{R_0}^R \beta_{RM}(\lambda, R') dR'}}{C_\lambda P_{t,\lambda} T^2(R) - 2S_A(\lambda) \int_{R_0}^R \frac{L_\lambda(R')}{T_{RM}^2(\lambda, R')} e^{-2S_A(\lambda) \int_{R_0}^{R'} \beta_{RM}(\lambda, R'') dR''} dR'} \right) \quad \dots(20)$$

Another change that should be made when considering the inversion from r_0 is that the initial pulse energy must also be scaled. This is done by multiplying the initial power $P_{t,\lambda}$ by $T_{RM}^2(\lambda, R_0)$ and setting it as the initial pulse energy.

4. SNR of the Lidar Receiver

The basic figure of merit for a lidar system is the signal to noise ratio (SNR). Other figures of merit, such as probability of detection and false

alarm rate, are functions of the SNR [10]. SNR is an important measure of the error present in the lidar return signal acquired by the three wavelength lidar instrument, which for the 532 and 355 nm channels of the lidar instrument can be expressed as [11]:

$$SNR^*(R) = \frac{I(R)}{\sqrt{4eBG \left(\frac{1}{1-\delta} \right) I(R) + \frac{4kBT}{R_L} + 4eBI_{dark}}} \quad \dots(21)$$

where $I(R)$ is the photocurrent at the anode of the PMT generated by photons scattered in (mA) from range R , e is the charge of an electron in (C), B is the bandwidth of the PMT in (GHz), G is the overall gain of the PMT, δ is the gain of an individual dynode stage of the PMT, I_{dark} is the dark current of the PMT (at the anode) in (nA), k is Boltzmann's constant in (JK⁻¹), T is the temperature in Kelvin and R_L is the load resistance in (Ω). The photocurrent $I(R)$ can be expressed as a function of incident optical power as:

$$I(R) = \frac{P(R) \lambda \nu G e}{hc} \quad \dots(22)$$

Where $P(R)$ is the optical power of light scattered by the atmosphere at range r , ν is the quantum efficiency of the PMT and h is Planck's constant. The signal to noise ratio is similar for the 1064 nm channel of the lidar instrument, and can be expressed as [12].

$$SNR^*(R) = \frac{I(R)G}{\sqrt{4eBG^2 F(I(R) + I_{dark}) + 4eI_{dark, nogain} + \frac{4kTB}{R_L}}} \quad \dots(23)$$

Where F is the excess noise factor, $I_{dark, nogain}$ is the dark current that is not multiplied by the gain and G is the gain of the APD. The photocurrent $I(R)$ can again be calculated using Eq (21).

According to Utkin et al. [13], the signal to noise ratio (SNR) of the lidar signal resulting from the accumulation of n_a lidar returns is given by the equation:

$$SNR1(R) = SNR^*(R) \sqrt{n_a} \quad \dots(24)$$

Signal to noise measurements show how well the desired signal can be distinguished from background noise. As the ratio of signal to noise approaches 1, the signal becomes difficult to distinguish from the noise.

5. Quantization Error

Quantization noise is added to the 355 nm, 532 nm and the 1064 nm signals when they are digitized so that they can be stored and analyzed via computer.

The digitization process consists of sampling the continuous voltage signal produced by the PMT and the APD at discrete time intervals, and rounding the voltage value of each sample to a discrete level that can be represented by the arbitrary number of bits used by the analog to digital (A/D) converter. The difference between the actual voltage value of the input signal from the lidar instrument and the discrete value assigned by the A/D card is the quantization noise.

The quantization noise is essentially uniformly distributed random (white) noise because the signals from the PMT and APD in the three-wavelength lidar instrument are usually within the range of the A/D converter and the quantization levels of the A/D card are uniform. The quantization process can therefore be modeled (in terms of the signal to noise ratio of the overall system) as adding uniformly distributed random noise to each sample. The signal to noise ratio associated with the quantization process that be modeled as [14].

$$SNR_2 = \frac{12 \times 2^{2t} \sigma_x^2}{X_m^2} \quad \dots(25)$$

Where SNR_2 is the signal to noise ratio resulting from the quantization process, $t+1$ is the number of bits used to represent the quantized data, σ_x^2 is the variance of the signal being quantized and X_m^2 is the range of the quantized input (the variance and the input range should use the same units; in the case of the three-wavelength lidar instrument the units are volt²).

Using the following equation to combine the signal to noise ratio of the optical receiver to the signal to noise ratio associated with the quantization process [15].

$$SNR = \sqrt{n_a \frac{1}{\frac{1}{SNR_1} + \frac{1}{SNR_2}}} \quad \dots(26)$$

6. Results and Discussion

Range resolved plots of the signal to noise ratio for the three wavelength lidar instrument calculated using Eqs (20-23) are shown in Fig. 2 for the 355nm, 532 nm and 1064 nm channels of the lidar instrument, respectively.

These signal to noise ratios were calculated using modeled atmospheric molecular backscatter profiles for each wavelength created using Eqs (11- 13).

Other values used for the calculation 1 for the overlap function and 1.5 m for the range resolution. As is expected, the signal to noise ratio decays exponentially with range, and is improved by averaging multiple lidar returns together. The signal appears more degraded at longer heights where the signal to noise ratio is worse. The signal becomes clearly in appearance as more returns are averaged together.

The signal to noise ratio associated with the quantization process are found to be 25, 24, 64dB for 355, 532, 1064nm channels respectively. This means that the noise introduced by the digitization process is significant when compared to the noise introduced by the optical detectors. In [16], The signal to noise ratio associated with the quantization process is on the order of 1020 and were neglected.

Using Eq (26) to combine the signal to noise ratio of the optical receiver to the signal to noise ratio associated with the quantization process for each channel, and is plotted in Fig. 3.

Figures (2) and (3) (c) of 1064 nm channel shows higher SNR with compared with 355 and 532 nm channels due to the using of (APD) detector which internally multiply the primary signal of photocurrent before it enters the following amplifier. This increases receiver sensitivity and the thermal noise is of lesser importance, so the optical detector noises usually dominated.

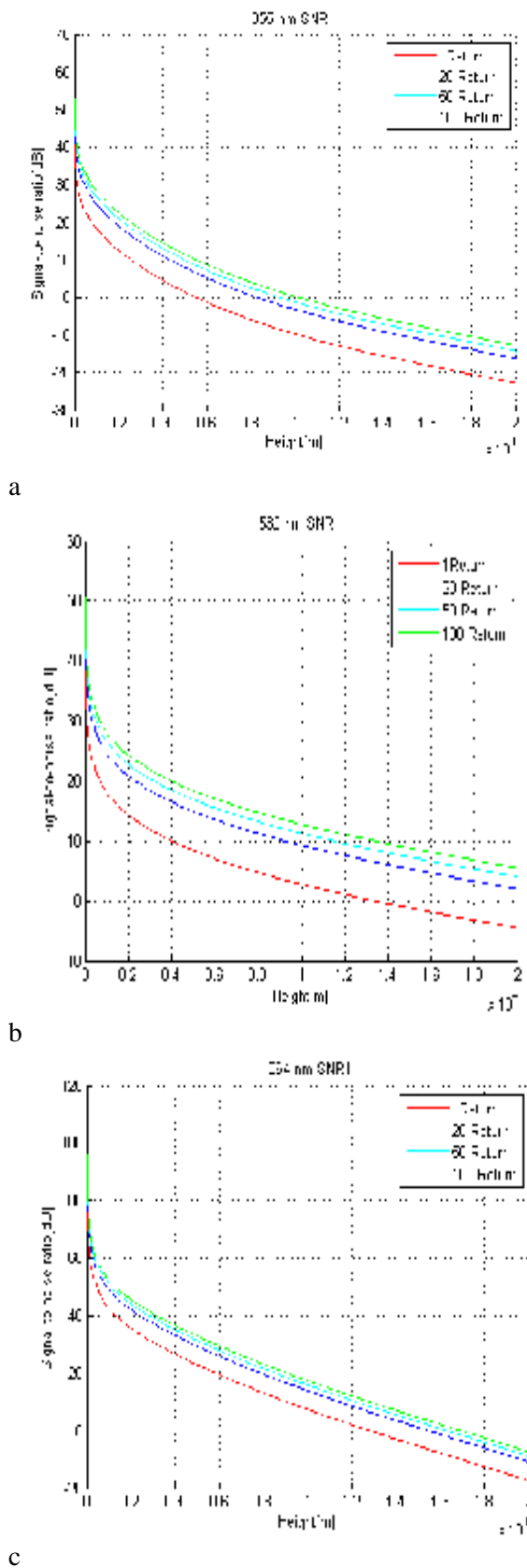


Fig. 2. A Plot of Signal to Noise Ratio of the Lidar Instrument While Averaging Together 1, 20, 50 and 100 Lidar Returns for (a) 355 nm Channel (b) 532 nm Channel (c) 1064 nm Channel.

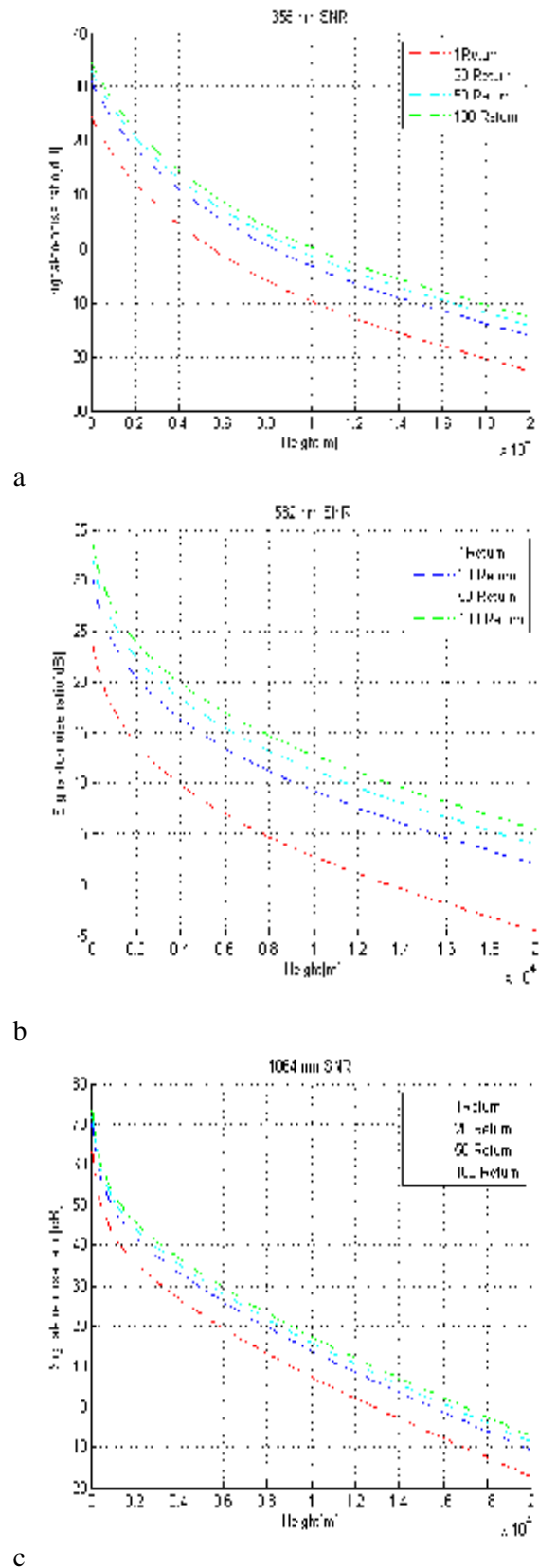


Fig. 3. Represents the Combination of Signal to Noise Ratio of the Lidar Instrument while Averaging Together 1, 20, 50 and 100 Lidar Returns for (a) 355 nm Channel (b) 532 nm Channel (c) 1064 nm Channel.

7. Conclusion

In this paper, a general method for the validation and performance measurement of three-color lidar system is proposed. We showed that the signal-to-noise ratio (SNR) of the lidar backscattering depended on the presence of aerosol layers and often attenuate rapidly due to noise and interferences, such as dark current, background noise, electronics readout noise and atmospheric turbulence. Although the quantization error was small but it cannot be neglected.

The range accuracy of a lidar system depend could not on signal bandwidth and the receiver signal-to-noise ratio (SNR).

8. References

- [1] V. A. Kovalev and W. E. Eichinger, *Elastic Lidar: Theory, Practice and Analysis Methods*. John Wiley and Sons, New York, 2004, p. 444.
- [2] C. Weitkamp, *Lidar: Range- Resolved Optical Sensing of the Atmosphere*, Springer, 2005.
- [3] D. S. Hoffman, A. R. Nehrir, K. S. Repasky, J. A. Shaw, and J. L. Carlsten, "Range-resolved optical detection of honeybees by use of wing-beat modulation of scattered light for locating land mines," *Applied Optics*, vol. 46, no. 15, pp. 3007-3012, 2007.
- [4] Yasser. Y. Hassebo, "Lidar Signal-to Noise Ratio Improvments Consideration and Techniques", Doctor of Philosophy in Engineering, The City University of New York, 2007.
- [5] Christian C. Marchant, "Retrieval of Aerosol Mass Concentration From Elastic Lidar Data", Doctor of Philosophy in Electrical Engineering, Utah State University, Logan, Utah, 2012.
- [6] Murray M. Regush, *Development of a LIDAR for Integration with the Naval Postgraduate School Infrared Search and Target Designation (NPS-IRSTD) System*, Master's Thesis, Naval Postgraduate School, Monterey, California, June 1993.
- [7] F. G. Fernald, B. M. Herman, and J. A. Reagan, "Determination of aerosol height distributions by lidar," *Journal of Applied meteorology*, vol. 77, pp. 433-448, 1989.
- [8] X. Wang, J. Reagan, C. Cattrall, and K. Thome, "Space borne lidar aerosol retrieval approaches based on improved aerosol model constraints," in *IEEE Workshop on Remote Sensing of Atmospheric Aerosols*, 2005, April, 2005, pp.36-42.
- [9] Benjamin D. Todt, "Use Of A Two Color Lidar System To Study Atmospheric Aerosols", Master of Science in Physics, Montana State University, 2010.
- [10] Michael S. Salisbury, Paul F. McManamon, "Signal to noise ratio improvement in lidar systems incorporating neodymium doped optical fiber preamplifiers," *IEEE Aerospace and Electronics Conference*, 1992, vol.3, pp. 1097 – 1103.
- [11] H. Corp., *High Speed Gated PMT Module H7680, H7680-01 Instruction Manual*. Hamamatsu Electron Tube Center, Japan, 2005.
- [12] *APD Module C5460SPL 6308 Instruction Manual*. Hamamatsu Solid State Division, Japan, 2007.
- [13] A. Utkin, "Effective platform for lidar fire surveillance", *Optics & Laser Technology* 41 (2009) 862–870.
- [14] A. V. Oppenheim, R. W. Shafer, and J. R. Buck, *Discrete Time Signal Processing*. Prentice Hall, Upper Saddle River, NJ, 1999, pp. 194-197.
- [15] M. Richharia, "Satellite Communication Systems- Design principals", McGraw-Hill, pp. 117-118.
- [16] D. S. Hoffman, "Two Wavelength Lidar Instrument For Atmospheric Aerosol Study", Master of Science in Electrical Engineering, Montana State University, 2008.

تخمين نسبة الاشارة الى الضوضاء متضمنة خطأ التكميم لمستقبل الليدار متعدد الأطوال الموجية

زينة عباس عبد* منى مصطفى حمادي**

**قسم هندسة المعلومات والاتصالات/ كلية الهندسة الخوارزمي/ جامعة بغداد

*البريد الالكتروني: baghdad_zaa@yahoo.com

**البريد الالكتروني: muna_hummady@yahoo.com

الخلاصة

يتناول هذا البحث تصميم وعمل محطة الليدار التي تعمل بعدة اطوال موجية. يعتمد هذا النوع من الليدار على ليزر النيديميوم ياك بطول موجي 1064 نانومتر والتوافقية الثانية بطول موجي 532 نانومتر والتوافقية الثالثة لليزر ذات الطول الموجي 355 نانومتر. نسبة الاشارة الى الضوضاء تعتبر من اهم عوامل قياس اداء الليدار خاصة اثناء العمل بالنهار كما وتعطي هذه النسبة مؤشرات مهمة في تصميم الليدار وكذلك في مدى عمل الليدار بسبب ما يوجد من ضوضاء في الجو وتداخلات تؤثر بشكل سلبي على النتائج المقاسة. تم تطوير خوارزمية الانقلاب في هذا البحث كما تم حساب نسبة الضوضاء الى الاشارة للقنوات الثلاثة (الأطوال الموجية الثلاث) لليدار عند جمع 1، 20، 50 و 100 من الاشارات المستلمة وجمع هذه النسبة مع خطأ التكميم وذلك لكل قناة من القنوات الثلاث لليدار.